Available online at www.CivileJournal.org

Civil Engineering Journal

Vol. 5, No. 4, April, 2019

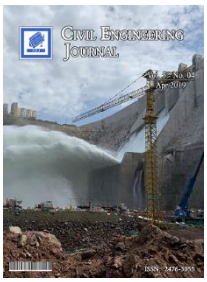

Design Charts for Axially Loaded Single Pile Action

Anis Abdul Khuder Mohamad Ali [a], Jaffar Ahmed Kadim [b], Ali Hashim Mohamad [c*]

[a] *Professor, University of Basra Department of Civil Engineering, Basra, Iraq.*

[b] *Lecture, University of Basra Department of Civil Engineering, Basra, Iraq.*

[c] *Graduate Research Student, University of Basra Department of Civil engineering, Basra, Iraq.*

Received 21 January 2019; Accepted 03 April 2019

Abstract

The objective of this article is to generating the design charts deals with the axially ultimate capacity of single pile action by relating the soil and pile engineering properties with the pile capacity components. The soil and are connected together by the interface finite element along pile side an on its remote end. The analysis was carried out using ABAQUS software to find the nonlinear solution of the problem. Both pile and soil were modeled with three-dimensional brick elements. The software program is verified against field load-test measurements to verify its efficiency accuracy. The concrete bored piles are used with different lengths and pile diameter is taken equals to 0.6 m. The piles were installed into a single layer of sand soil with angles of internal friction (20° t0 40°) and into a single layer of clay soil with Cohesion (24 to 96) kPa. The getting results showed that for all cases study the total compression resistance is increased as pile length increased for the same property of soil, also illustrious that the total resistance of same pile length and diameter increased as the soil strength increasing. In addition, the same results were obtained for the end bearing resistance, skin resistance and tension capacity. Design charts were constructed between different types of soil resistance ratio and the pile length/diameter ratio (L/D) for all cases of study. One of improvement found from these curves that it is cheaply using piles of larger diameter than increasing their lengths for dense sand and to increasing piles lengths for loose sand. Moreover, it is inexpensively using piles of larger length in soft clay soil than increasing their diameter and piles of larger diameter in firm and stiff clay soils than increasing their length.

Keywords: Pile; Compression Load; ABAQUS Program; Design Charts; Pile Action.

1. Introduction

Piles defined as a slender long columns put in into the ground to utilized for transferring applied toad (vertical, horizontal, uplift) to stronger soil layers. Piles were usually used to reduce a large settlements of constructions structures that occurred by shallow foundations due to the soil void rate [1]. Also, piles were widely used in many buildings and structures such as basement mats, offshore platforms, transmission towers, piers an abutments of bridge, and etc. For vertical load resistance, piles can be categorized as a friction (flouting) piles or an end-bearing piles. But this classification has questionable remark for piles utilized in transmitting by a collection of the end-bearing and side friction portions. Tomlinson (1995) proposed a simple classification founded on the British Normal Program (BS 8004) of Repetition for Foundations [2].

Many methods had been developed during past decades by different researchers to find accurately the ultimate pile capacity such as Winker method, plasticity theories, numerical methods, an etc. But all of these methods have an

* Corresponding author: ali.eng9851@gmail.com

http://dx.doi.org/10.28991/cej-2019-03091300

approximate nature according to the omitting or ignoring some aspects of the variables which controlling the behavior of problem domain (pile, soil, force transfer, force component of pile). To illustrate some of the above methods, below a number of researchers work are given as follows:

Coyle et al. (1966) [3] used load transfer method, which involves an iterative analysis procedure. The procedure relies on curves which relate the ratio of load transfer to soil shear strength versus pile displacement along the length of the pile. The curves are constructed from data obtained from the field or laboratory-instrumented piles.

Goodman et al. (1968) [4] was the first in the field of rock mechanics to apply a special two dimensional joint elements and combining their rigidity to the structure global stiffness. This method has developed to symbolize the jointed rock masses behavior. The element of joint was presented as an one dimensional simple tube, with eight freedom grades represent the translation freedom degree, offering resistance to shear and compressive forces acting along parallel and normal direction to its axis.

Randolph et al. (1978) [5] produced an approximate analytical solution for a rigid pile by considering separately the load sustained by the pile shaft and the load sustained by the pile base. They assumed a uniform shave stress circulation alongside heap shaft, and the normal stresses beneath the pile base as those of arising from a rigid punch at the surface of an elastic half space.

Laethem et al. (1983) [6] used a combined boundary element and finite element methods to represent SSI in two and three dimensional analyses, the region near the applied load which behaves as non-linear are modeled as a finite element while the far end are represent by a boundary element, which is used to model the elastic behavior of far field.

Eduardo et al. (1999) [7] presented an obvious finite element method for determining load-settlement history of axially loaded skin friction piles in linear range. The method is based on an exact analytical solution of the differential equation governing the behavior of skin friction piles. A fourth order polynomial is used to fit the soil resistance distribution along element length.

McCabe et al. (2006) [8] dealt with a case history involving to the five pile capacity classified as closely spaced, precast concrete piles casted in a soft clay-silt that made throughout the installation in addition to load testing regarding of pile groups. The maintain full compression test scale and tension load test on groups, in addition to tests achieved on indication single piles including to an individual test on a pile inside a pile group, were be used to be assessed the facilitated the estimation of these effects of multiple pile installations and interaction between piles under load. The results ha to be assessed been compared with the accessible simple methods of pile group analysis furthermore with other reporting results of case histories on small pile groups. A straightforward expression to evaluate pile group stiffness efficiency was proposed.

Lashkari (2012) [9] projected a simple semi-hyperbolic state-dependent constitutive model communicated to sand-structure interfaces. The model had been formulated by consisting the soil mechanics of critical state given that the continuous devolvement of void ratio with shear strain that has a movement from an initial state towards asymptotic critical state at extremely large shear strains. The model concerned the effect of normal stiffness on volume change in addition to stress path, and interface model in a pile performance. Results had been showed that the analysis of the proposed pile segment was a good indication for the prediction of the pile shaft resistance, side friction, which embedded in different sandy soils.

Dong-dong et al. (2017) [10] studied the interactive effects amongst the group piles via the shear displacement method using the principle of superposition. The displacement of single pile shaft at a given depth was understood to be composed of the soil-pile comparative displacement that developed at the disturbed soil which surrounding pile and the elastic vertical displacement of soil urbanized during soil mass. A new load-transfer function (hyperbolic model) had been constructed to clarify the relationship between the unit skin friction of pile and its shaft displacement by a given depth. In the same way, the hyperbolic model was used to imitate the association between unit end resistance of pile and pile end displacement. The results of the proposed method was checked with the measured results and the estimated values consequential from further methods.

Shengyang et al. (2017) [11] considered the settlement of piles in soft soil by introducing a suggestion model to involve both the pile shaft nonlinearity based on visco-elastic and the $(t - z)$ models of pile load transfer of the modified model of Burgersby substituted its spring as a hyperbolic model. For these models, the developed a nonlinear came closer to estimate the settlement (time-dependent) occurred of a vertically loaded single pile and pile groups in layered soft soil. Parametric studies had been achieved to examine the effect of these parameters on the single pile settlement so that this settlement was confirmed to a single pile by an instrument pile loading test.

Hasan et al. (2018) [12] investigated the interaction in the pile-soil-pile in a pile group for battered piles. The effect of a little spacing between piles on the group or one to another using the interaction between them had been examined. The interaction of battered piles in a group was numerically modeled using finite element method analysis so both the frictional and frictional double pile groups under static lateral and axial loadings were analyzed independently. The

property of parameters on interaction factors such as the pile–soil stiffness ratio, batter angle, slenderness ratio, spacing between piles, and soil plasticity had been estimated and obtainable in an appropriate curves.

Tiago et al. (2018) [13] made two modifications to the load-transfer technique of traditional formulation using a distinct unloading path that define the load-transfer functions. Also, the displacement variable was modified to regard as the effects of passive soil displacements. The formulation used can description for most dissimilar properties all along the pile depth such as the case of various soil layering. The different modeling of unloading functions enables the loading cycles to be imitation as well as the analysis of residual loads. An instrumented pile load test had been used to calibrate the method. Examples calculation are offered and discussed the highlighting of the major features of the studied model

Md. Nafiul Haque et al. (2018) [14] offered the analyses of twelve pre-stressed concrete instrumented test piles that driven in different bridge construction projects of Louisiana in order to develop an analytical models for estimating the increase in pile capacity with time as known a pile setup. These test piles had been mainly driven in cohesive soils. Comprehensive soil characterizations counting laboratory and in situ tests were conducted to conclude the various soil properties. The test piles were instrumented with vibrating wire strain gauges, piezo-meters, pressure cells that were monitored throughout the whole testing period. Several static load tests and dynamic load tests were conducted on each test pile at different times after end of driving to calculate the pile capacity magnitude and rate of setup.

Yunlong (2019) [15] made assessment method of load transfer mechanism for piles in unsaturated expansive soils as they designed by another way than conventional design procedures of saturated soils. He developed a simple methods to predict the load transfer mechanism changes of piles in the expansive soils upon infiltration in which more importance was heading for the calculation of the pile performance. The model included three parameters that given as the load-displacement relationship of pile head, the axial pile force (shaft skin or friction) distribution, and the pile end bearing (base resistance) using unsaturated mechanical as a solver tool. The proposed modified shear displacement method together with the modified load transfer curve method were being a simple and necessitate a limited number soil properties including the metric wetting and drying suction profile upon, characteristic curve of soil water, and some physical properties of soil.

Psaroudakis (2019) [16] analyzed work of single pile behavior which submitted to axial loading. He examined the static stiffness coefficient at the head of a flexible pile, vertically embedded in a homogeneous or multilayer soil of random geometry, and the mechanical properties. For solving the problem, Winkler's theory was used to develop an analytical closed form. The model had been used in combination with appropriate shape functions that described the consistently the vertical movement of the pile all along the depth. Choosing the suitable shape functions along with "t–z" and "q–z" curves and following an iterative process, a relatively accurate estimation of the vertical displacement at the head of the pile had been achieved. Distinct traditional numerical solutions, the method proposed did not required discretization of the pile into finite elements but only discretization in sections aiming integration with depth.

2. Mechanism of Load Transfer

When compressive load is applied on pile head, then pile head will have settled and the corresponding curve of load-settlement will result as presented at Figure 1(a). The soil-pile scheme initially works elastically up to point A, after that the curvature take place continued to reach point B which being the highest friction. When load releasing, the curve takes a straight line pattern to point C in which the distance OC known as "permanent set". As the reloading begin, the curve behaves a nonlinear until point E and beyond this point a large curvature is happened until Point D so that no further loads is resist by pile [2].

The compression load is resisted by two pile actions, the first one is by the side pile surface, sometimes is referred as skin resistance or friction resistance as indicate in Figure 1(b) which appear the pile transfer the load to the soil in every step of loading appeared at Figure 1(a). The second action is achieved by the end pile area which well known as the tip point action or sometimes end bearing action.

Therefore, when a pile is overloaded till point A basically the total load is supported via friction on the shaft of heap and there's no or little transferrable of load to the pile toe (as appear in Figure 1.b). When the applied load arrives to B the shaft of the heap will carry its greatest frictional confrontation then also the toe of the pile will carry roughly of the load. On D the base capacity will arrive its critical value and no more rise in the load which is transported in friction. Typical load/settlement curves shown in Figure 2 for a compressive load of the total load capacity (Q_t) and the base load capacity (Q_b)and the shaft load capacity (Q_s) typical reliant on stratums of soil as Figure 2(a) shown a friction heap while Figure 2(b) show an end-bearing heap [17].

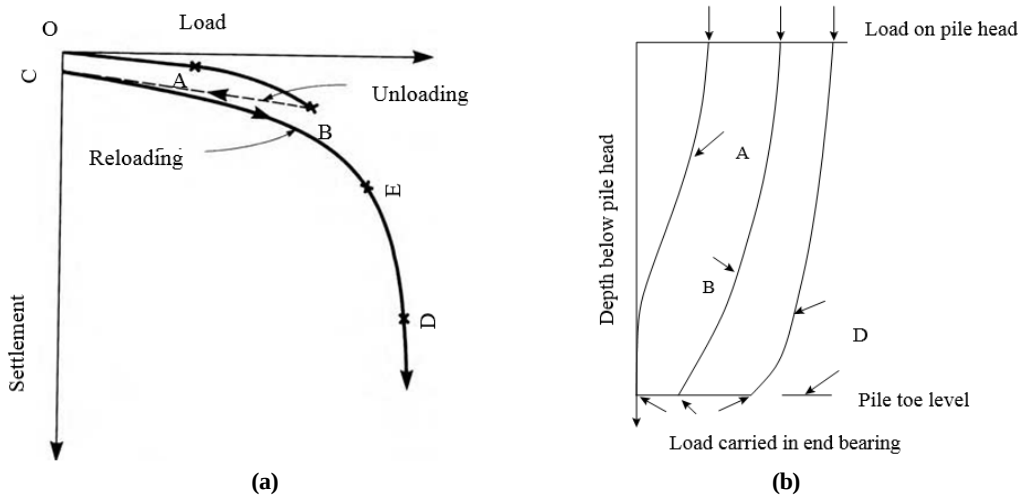

Figure 1. Load transfer from head of pile with corresponding settlement, (a) Load/settlement curve for pile compressive load to failure, (b) Load transfer to shaft at points A, B, and D

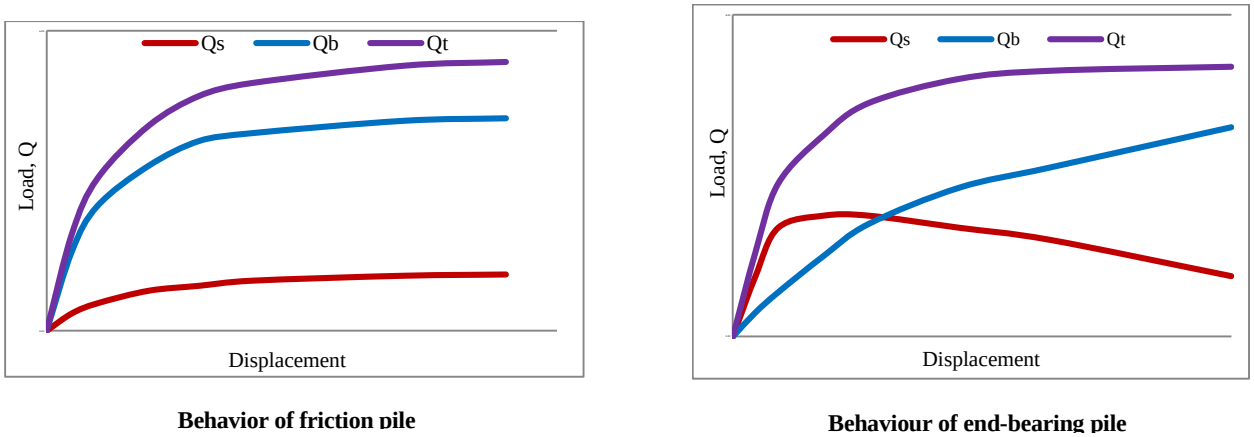

Figure 2. Typical load/settlement curves for compressive load tests: a) friction pile; (b) end-bearing pile

The target of this study is to assembly the soil and pile engineering properties together with pile load components in single chart by considering different analyffiguresis stages and to achieve this proposed target the finite element method via ABAQUS program is utilized to generate these design charts of single pile action which loaded in the axial direction (compression or tension). In the first, the method used in constructed these charts are compared with field measurements to find the degree of compatibility between them. These curves depend on the engineering properties for both the pile and soil and they give the ultimate pile capacity at failure and the contribution of pile components i.e. the shaft resistance and end bearing.

3. Research Methodology

In present work, the problem domain involve three types of different element materials which are the pile, soil, and the interface material which has different engineering properties for each one as shown in Figure 3 and therefore they have a different structural behavior – response under the action of forces and applied loads.

3.1. Pile Formulation

The pile was modeling by using twenty node brick element in this study [17] which formulated by a linear elastic model because in most real situation the failure of piling foundation occurs in the weaker materials i.e. the soil element. This element is more capable and more accurate for modeling problems with curved boundaries than the eight-node brick element. According to the Hook law, it simply offers two input factors, that is, Poisson's ratio and Young's modulus to achieve the pile formulation. For briefly, the search will not include the equations and related modeling which used for the formulated of pile that are amiable in the relevant topics.

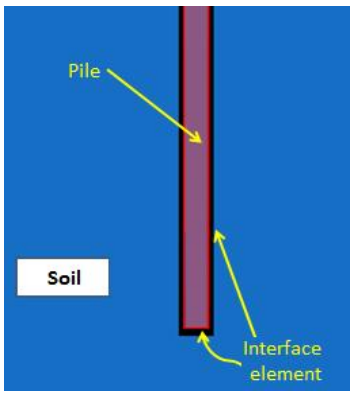

Figure 3. The model of domain (pile, soil, and interface element)

3.2. Soil Formulation

For soil formulation, the elastic-plastic model, considering the Mohr-Coulomb model, was used on the soil failure simulation because it is suitable model in practical states which was recognized by including the internal friction angle and the cohesion intercept to determine the whole stress-strain performance.

Mohr-Coulomb condition adopts that yield is organized by the full shear stress and this yield shear stress be subject to the normal stress. This could be characterized through scheming Mohr's circle for stress conditions on yield in relations of the minimum and maximum main stresses. The failure line of Mohr-Coulomb is the finest traditional line that drops these Mohr's circles, as in Figure 4. Therefore, the Mohr-Coulomb principle thus, the Mohr-Coulomb criterion can be written as can be inscribed as [18].

$$\tau = c + \sigma \times \tan \emptyset \quad (1)$$

$$\frac{\sigma_1+\sigma_3}{2} \sin \emptyset - \frac{\sigma_1-\sigma_3}{2} - c \cos \emptyset = 0 \quad (2)$$

Where (σ) is the normal stress, (c) is the material cohesion, (τ) is the shear stress, and $(\emptyset)$ is the friction angle of material.

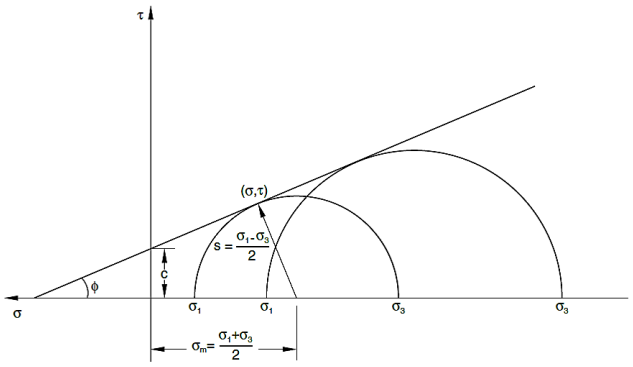

Figure 4. Mohr-Coulomb failure criterion

3.3. Interface Formulation

There are two different interface element types which used to formulation the pile-soil interaction in which the first one known as the tangential interface element applied to represent the pile-soil interaction at shaft pile area while the second type defined as the only compression element which practically used to capture the pile-soil interaction at the remote pile.

The first interface element formulation was utilized in the numerical investigation of soil–structure major changed in the continuity due to materials changes such as structures and surrounding soils. The interface part is formulated as three dimensional elements which are divided into two types, the first one is side element in which it consists of two normal stresses and one shear stresses as depicted in Figure 5.a [4, 19] and this type is capable to take one tangential movement (up and down) along pile shaft and two normal movements.

The second type is known as end (Tip Point) bearing which has only normal stress (sometimes called only compression element) that is capable of supporting axial compression loading only as shown in Figure 5.b. This bearing element is performed as a nonlinear spring element that present to income into excuse the interface among the soil and end pile. If the pile has tensile stress then zero stiffness value had been assigned to it.

3.4. Solution of the Problem

The formulated problem involved into two types of nonlinearity aspects which can be came from the physical nonlinearity (soil material and interface) and the geometrical nonlinearity (pile). In material nonlinearity, the connection among strain and stress is a complex nonlinear occupation which produce quantities dependent on the answer. Geometrical nonlinear results from finite changes in geometry of the deforming body. To solve this problem, ABAQUS software was adopted here which has the advantages to solve the problem with strong nonlinear and discontinuous property. The final model of current problem is shown in Figure 6.

To find the required solution, the next steps are employ as follows:

- The pile properties and geometry are specified fixed and they include pile diameter, length, density, elastic modulus, and Poisson ratio.
- In the similar manner, the soil properties are given which involved soil density, elastic modulus (related to soil cohesion), Poisson ratio, and angle of internal friction.
- Soil boundaries are established so that zero displacement are assigned to it.
- Interface properties are assigned like pile and soil processes.
- The load is applied in incremental manner so that for each load step the whole analysis was carried to find the pile force components with pile head displacement. This operation is continued until no further load is resisted by pile i.e. displacement at pile head increased without increasing applied load. At this stage the last load is considered the ultimate pile capacity.

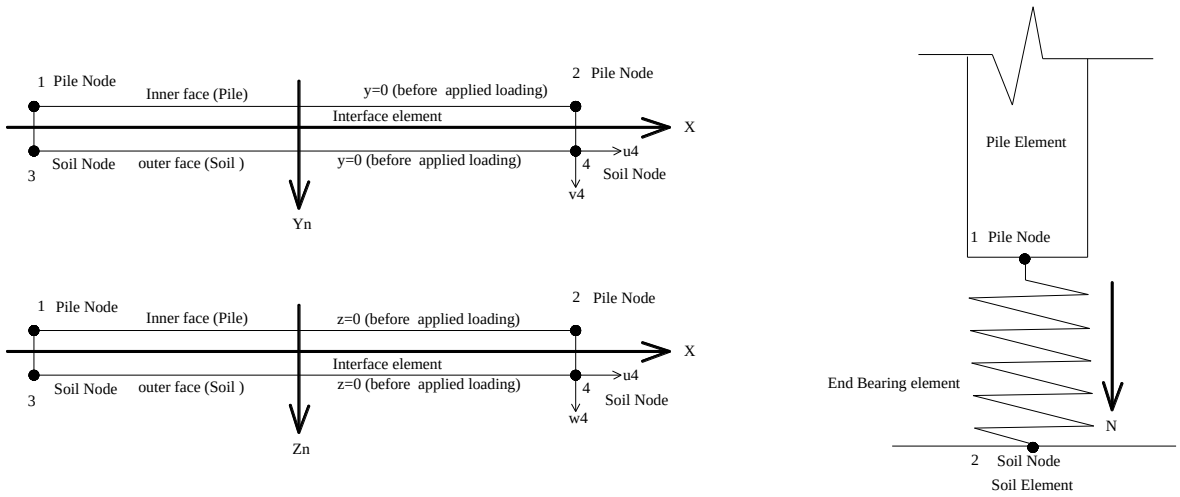

(a) Side Interface element **(b) End bearing interface element**

Figure 5. Interface Element Types

5. Verification Case

The computer program is verified against real behavior through making comparisons between the computed and the measured results obtained from field tests (pile load test) from a case study. These comparisons are presented in terms of the relationships between the applied axial loads and the pile head settlement. The reference data in this study are soil investigation and pile load test results for Majnoon gas project in Majnoon oil field, southern Iraq [20]. The piles were tested according to ASTM D1143 method for bored concrete piles as shown in Figure 7. The finite element prediction (present study) shows satisfactory comparisons with field test with the selected verification problems as degree of compatibility equals to 99% at failure load which it controls the design of piles. One of the most important point associate with load transfer is the combined action of pile side friction and end bearing as mentioned in Figure 7.

It is found from the pile load test curves that the FEM model is closer to the real behavior near the failure portion than the initial curve, this reflects the following two important facts:

1. The first portion is more sensitive to the adjustment to force distribution to the test plates which make some disturbance at the beginning of the test.
2. There are a great match not in the quantity between FEM and PLT but also in the quality behavior near failure zone.

The finite element prediction (present study) shows satisfactory comparisons with field test with the selected verification problem. Therefore, ABAQUS package could be used here with satisfactory accuracy.

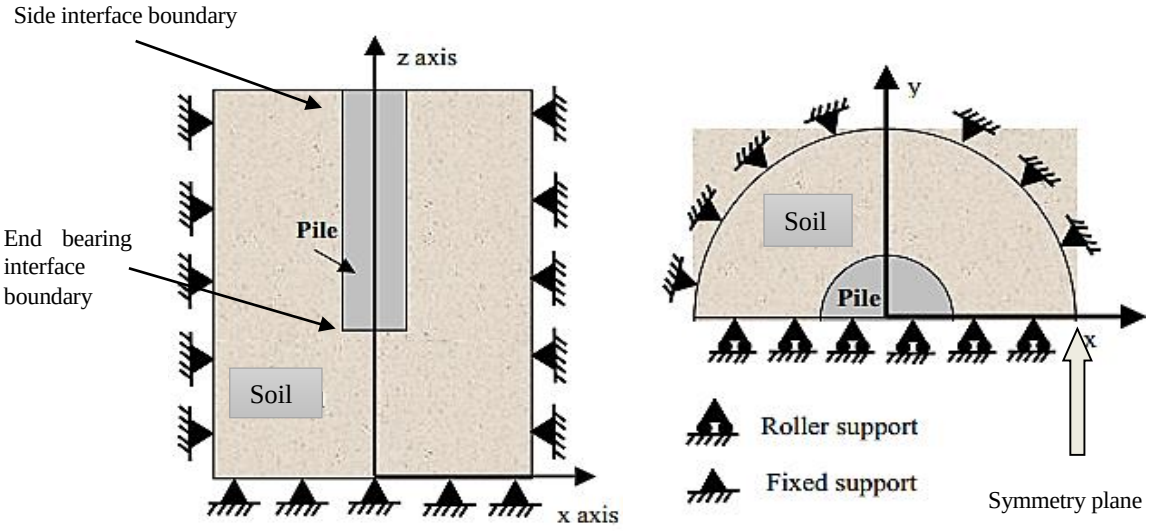

(a) Front view **(b) Top view**

Figure 6. Boundary condition in the symmetry plane and other edge of the model

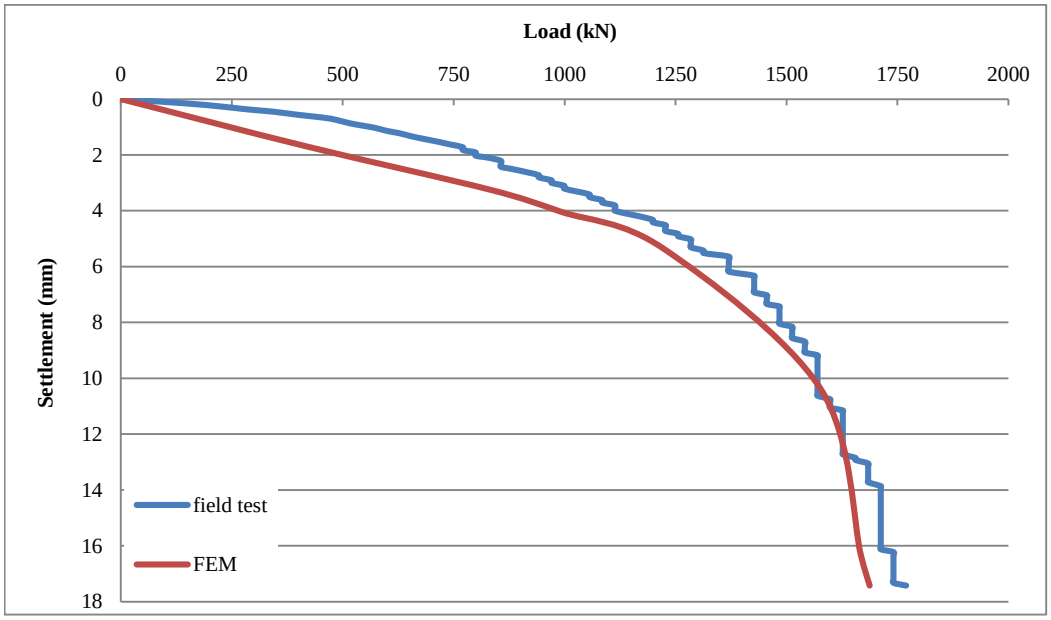

Figure 7. Comparison of Load-settlement curve between field load test and ABAQUS results for bored pile for failure static axial load equal to 1765.197 kN

6. Results and Discussion

This section focuses on the concrete bored piles than precast piles, one of the reasons related to the huge domain applications of the bored pile dimensions' variations (pile length and pile diameter) in different projects than the precast concrete piles which found by predefined limited dimensions (0.3×0.3) m or (0.4×0.4) m. The pile diameter is usually ranging from 0.6 m to 1.5 m but frequently taking 0.6 m in most projects, therefore in present work this value is taken as 0.6 m as a reference in the design charts. The second reason related to the pile bearing capacity which in the bored concrete piles reach many times greater than the precast concrete piles.

6.1. Axially Loaded Single Bored Piles in Sand

A bored pile which it's properties are shown in Table 1 was installed into a single layer of soil (sand only), five types of sand have been used their properties shown in Table 2 [59]. The pile was loaded axially (compression and tension), and the results of the analyses give the ultimate capacity of the pile for the compression and tension loads. In order to construct the design curves of the piles studied here, the following parameters are used as defined as following:

L= Pile length (m), D= Pile diameter (m), Ft= Total compression pile resistance or ultimate load of pile capacity (kN), Fb= End bearing pile resistance or base resistance (kN) for compression load only, Fs= Side or skin friction pile resistance (kN), Ften=Tension pile capacity (kN), Ø= Angle of internal friction, K= Modulus of sand subgrade reaction (kN/m³), L/ D= Length pile ratio, (Fb/Ftx100)%= End bearing percent ratio (%), (Fs/Ft)%= Skin resistance percent ratio (%), End Bearing Parameter=Fb/(kDL^2), Skin Resistance Parameter=Fs/(kDL^2), Compression Resistance Parameter= Ft/(kDL^2), Tension Resistance Parameter= Ften/(kDL^2).

Table 1. Types and properties of concrete piles in this study

Properties	Bored pile
Young's modulus (E), MPa	25 000
Poisson's ratio (υ)	0.16
Unit weight (γ), kN/m^3	24

Table 2. The properties of sand soils

Modulus of Elasticity (MPa)	Poisson's ratio (υ)	Cohesion (kPa)	Angle of Internal Friction (Ø)	Density (kN/m³)
20	0.3	0	20	18
30	0.3	0	25	19
40	0.3	0	30	20
50	0.3	0	35	21
60	0.3	0	40	22

The pile with different length (12, 14, 16, 18, 20) m was analyzed and load- settlement curve was obtaining for each length regardless the compression or tension load case and then the failure criteria the ultimate load was found until it was reached the failure criteria t find the ultimate load for the pile as previously defined for the pile as previously defined, the results are shown in Table 3 the associate result are drawn in Figures 10 to 17.

From Table 3 it is so clearly that in loose sand the pile capacity depends on side friction (66% average over length) resistance than the end bearing (34% average over length) while for dense these ratios become side friction (33% average over length) resistance than the end bearing (67% average over length). These results can be attribute to the effect of great change in soils strength parameters which alter the pile strength components so that an important fact is obtained that is the trend of pile resistance type from friction to end bearing mainly related to sand soil type other than pile length. Moreover, Table 3 shows that the pile capacity were controlled by dual action of side an end pile for selected dimensions regardless of strength value, therefore is not practical consideration to assume the pile in sand soil behave as end bearing pile.

From Figure 10 it is noted that the end bearing% {(62-71) for the dense sand and (31-35) for the loose sand and other sand types lies within above range values} value at the same pile length increase as the soil strength increasing, therefore the skin resistance% {(29-38) for the dense sand and (65-69) for the loose sand and other sand types lies within above range values}is decreasing as the soil strength increasing at the same pile length as shown in Figure 11. It is depicted from last two figures that the shaft resistance become larger value and end bearing lesser value as pile length increased regardless soil strength and this result came from the contribution of pile length in side friction other than end bearing resistance.

Figure 12 showed the variation of total resistance which is increased as pile length is increasing for the same property of sand soil which indicate the total resistance at same pile length increase as the soil strength increasing but with the same performance as the soil strength changed. And the same situation for Fb and Fs as shown in Figures 10 and 11.

Figures 13 to 15 showed the same tendency of pile resistance parameters with enlarged length pile ratio in which all pile strength parameters reduced their values but maintain their performance as soil type changed. These results indicated a new facts associated with the design chart that giving a unique model of pile behavior with different coefficients used in developed these charts for derivative the proposal mathematical expression equation in further studies.

Figure 16 display the same trend of tension pile capacity with increasing pile length in which the soil strength shifted the relation line to above without changed its shape. Also, the tension resistance parameter in Figure 17 is more sensitive to soil strength in loose type, reduce with pile length ratio, than dense.

6.1.1. Important Results Regarding Sandy Soils

The obtained results reveal two important notes. The first one related to compression load of pile that the increasing of pile length causes a decreasing in the end bearing ratio for dense and medium sand soils types and increasing for loose sand and this result can be explained that the increase in pile length will cause an increase in the friction side area of pile shaft leading to growing the skin resistance force other than the end bearing resistance. Therefore, it is economically to use piles of larger diameter than increasing their lengths for dense sand and to increasing piles lengths for loose sand. The second point is the end bearing results show the assumption of the end bearing controlling the capacity of pile in sand soils is a questionable remark especially for loose to medium sand soils (the friction portion is larger than end bearing portion) and consequently it is valid approximately for dense sand of short length (L/D less 15) after that the behavior of piles in all sand soils become a friction-bearing actions which control of the pile analysis and design.

Table 2. The results for the variation of different soil resistance types with pile length increasing of pile diameter equals to 0.6 m in sand

Soil	L	Ft	Fb	Fs	(Fb/Ft) %	(Fs/Ft) %	Ften
Ø=20 K=3.0 MN/m³	12	761.00	240.00	521.00	31.5	68.5	546.92
	14	935.42	301.27	634.15	32.2	67.8	664.39
	16	1142.64	397.96	744.68	34.8	65.2	779.24
	18	1341.52	464.76	876.77	34.6	65.4	915.65
	20	1592.11	558.74	1033.37	35.1	64.9	1076.57
Ø=25 K=4.0 MN/m³	12	996.18	385.88	610.30	38.7	61.3	636.22
	14	1202.99	428.60	774.39	35.6	64.4	804.63
	16	1439.98	511.76	928.22	35.5	64.5	962.78
	18	1605.02	591.72	1013.30	36.9	63.1	1052.18
	20	1865.83	662.35	1203.48	35.5	64.5	1246.68
Ø=30 K=6.8 MN/m³	12	1240.40	514.88	725.52	41.5	58.5	751.44
	14	1576.50	655.41	921.09	41.6	58.4	951.33
	16	1882.88	779.22	1103.66	41.4	58.6	1138.22
	18	2123.96	885.12	1238.84	41.7	58.3	1277.72
	20	2316.17	926.55	1389.62	40.0	60.0	1432.82
Ø=35 K=24.4 MN/m³	12	2096.90	1324.10	772.80	63.1	36.9	798.72
	14	2400.91	1427.76	973.15	59.5	40.5	1003.39
	16	2789.84	1594.21	1195.63	57.1	42.9	1230.19
	18	3076.25	1752.40	1323.85	57.0	43.0	1362.73
	20	3484.54	1982.56	1501.99	56.9	43.1	1545.19
Ø=40 K=61.0 MN/m³	12	3034.37	2151.89	882.48	70.9	29.1	908.40
	14	3397.60	2352.46	1045.14	69.2	30.8	1075.38
	16	3880.94	2609.04	1271.90	67.2	32.8	1306.46
	18	4093.12	2689.93	1403.19	65.7	34.3	1442.07
	20	4387.13	2728.31	1658.82	62.2	37.8	1702.02

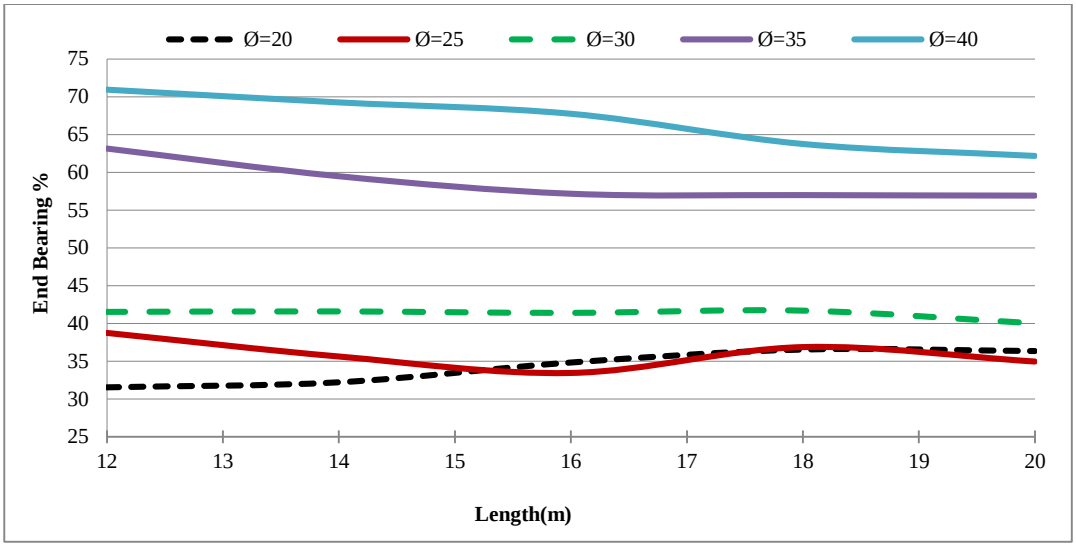

Figure 10. Relationship between end bearing % and pile length in sand soil

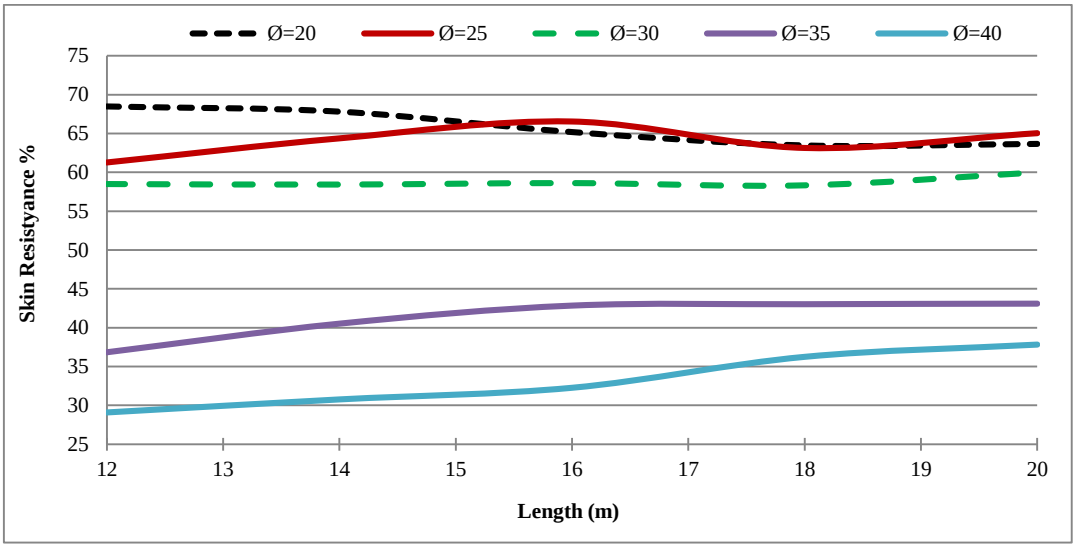

Figure 11. Relationship between Skin Resistance% and pile length in sand soil

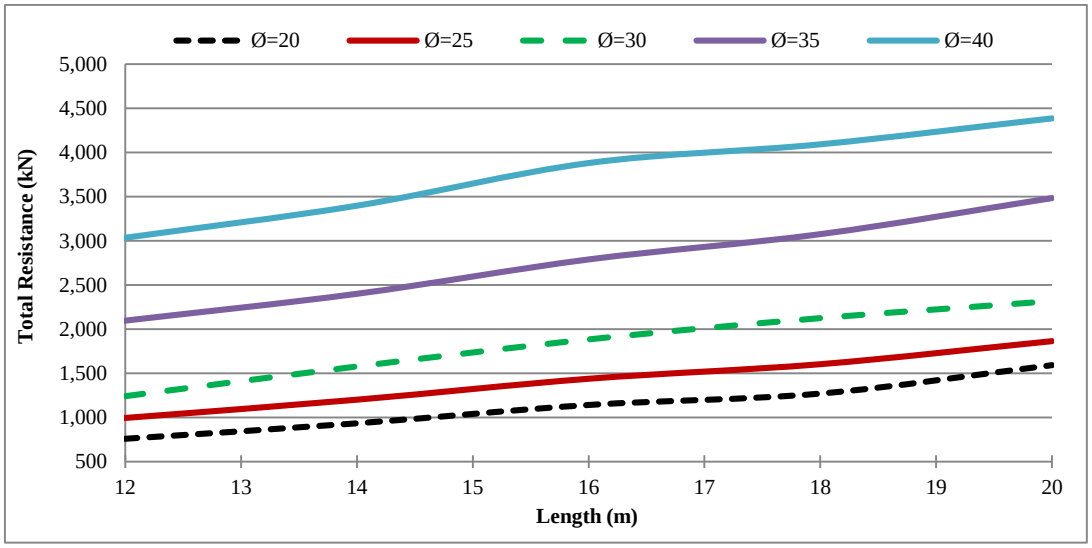

Figure 12. Variation of total resistance with pile length in sand soils

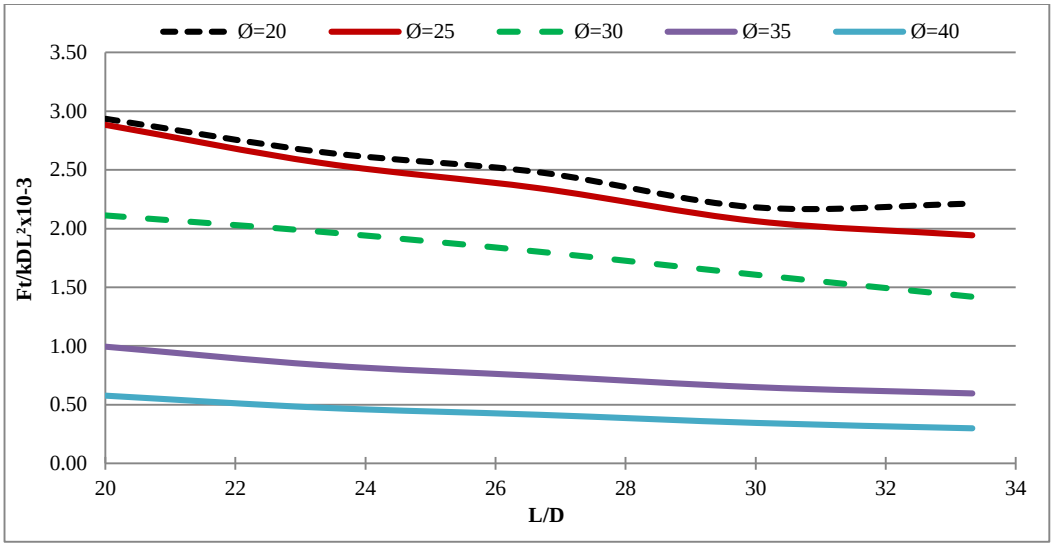

Figure 13. variation of total resistance ratio with L/D in sand soil

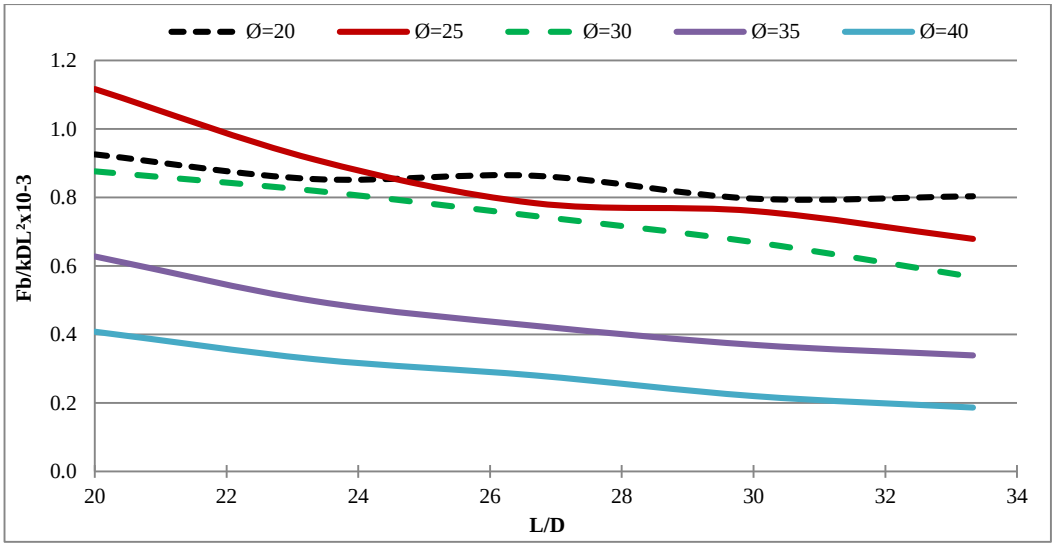

Figure 14. Variation of end bearing resistance ratio with L/D in sand soil

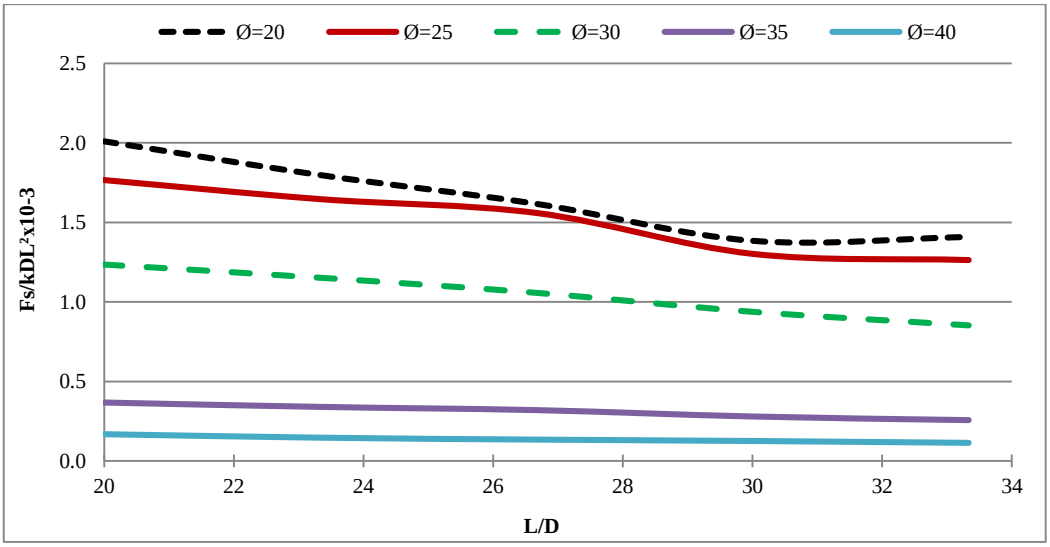

Figure 15. Variation of skin resistance ratio with L/D in sand soil

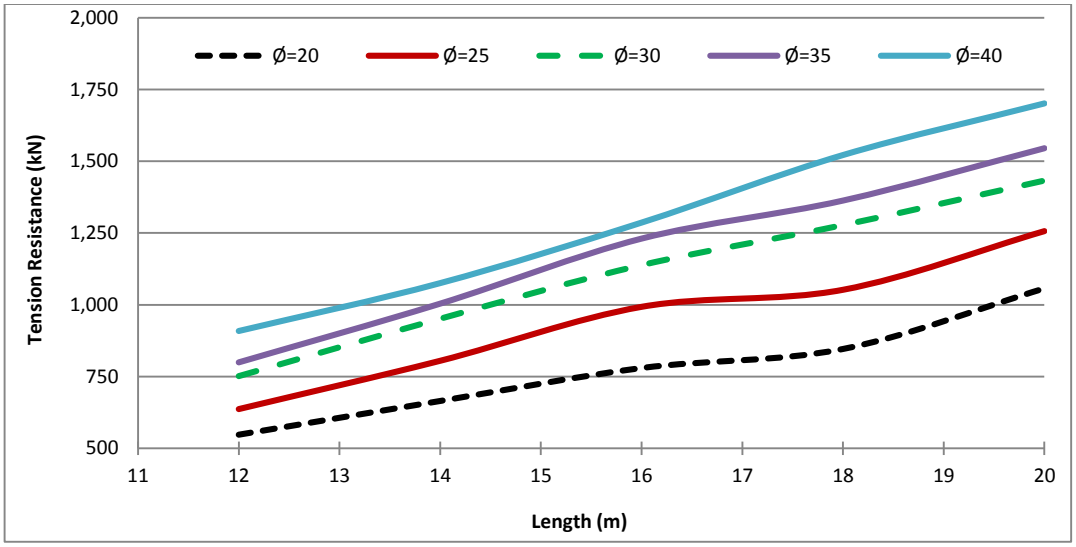

Figure 16. Variation of tension resistance with pile length in sand soil

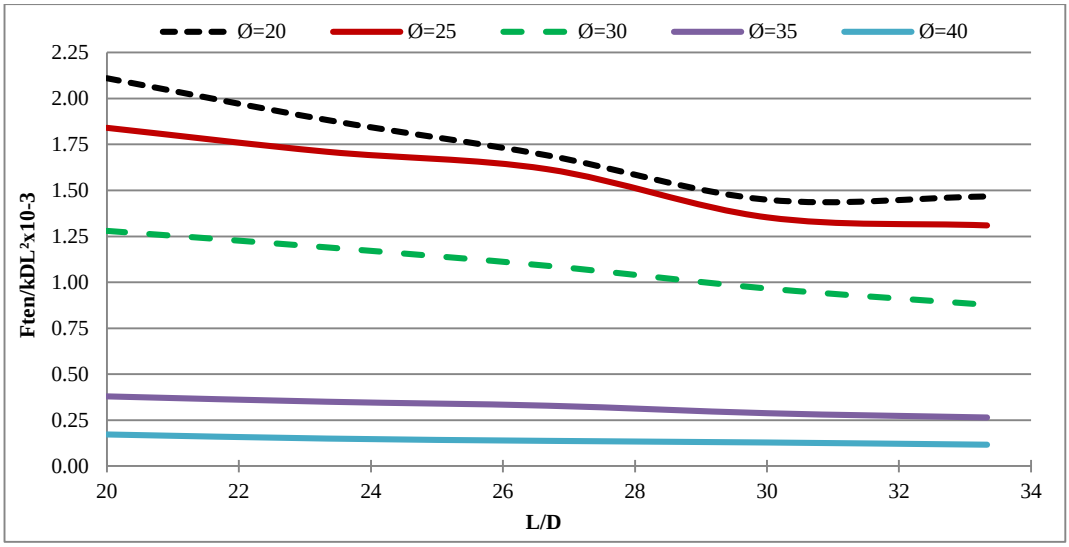

Figure 17. Variation of tension resistance ratio with L/D in sand soil

6.2. Axially Loaded Single Bored Piles in Clay

The same bored pile which shown in Table 1 was installed into a single layer of soil (clay only), three types of clay have been used their properties that shown in Table 4 in which these selected values for soil properties represent the strength values range (soft, firm, stiff) clay in the most practical situations. The pile was also loaded axially (compression and tension), and different soil resistance types were obtained. To construct the design curves of piles in clay soils, the definitions in previous section are used here, the additional parameter is the strength parameter that equal to ratio between the specified piles resistances divided by the external pile dimensions multiplied by soil resistance expressed as the soil cohesion. Therefore, there are four specified strength parameters used which are defined as follows:

End Bearing Parameter=Fb/(CuxDL), Skin Resistance Parameter=Fs/(CuxDL), Compression Resistance Parameter= Ft/(CuxDL), Tension Resistance Parameter= Ften/(CuxDL), where Cu= Soil Cohesion (kN/m²).

Different pile lengths (12, 14, 16, 18, 20 m) were used that have been modeled and analyzed, and the results of compression and tension load with pile length increasing are shown in Table 5 which indicate a reduction of shaft resistance as pile length is increased and a dissimilar effect is found for end bearing resistance. The results of soil resistance ratio with length/diameter pile ratio are drawn in Figures 18 to 25.

Table 4. The properties of clay soils

Modulus of Elasticity (MPa)	Poisson's ratio (υ)	Cohesion (kPa)	Angle of Internal Friction (Ø)	Density (kN/m³)
12 (soft)	0.49	24	0	18
24 (firm)	0.45	48	0	20
48 stiff)	0.4	96	0	21

Table 5. The results for the variation of different soil resistance types with pile length increasing of pile diameter equals to 0.6 m in clay

Soil	L	Ft	Fb	Fs	(Fb/Ft) %	(Fs/Ft) %	Ften
Soft Cu = 24	12	619.59	88.36	531.23	14.3	85.7	557.15
	14	769.59	125.60	643.99	16.3	83.7	674.23
	16	930.63	165.50	765.13	17.8	82.2	799.69
	18	1076.07	199.50	876.57	18.5	81.5	915.45
	20	1219.34	259.32	960.01	21.3	78.7	1003.21
Firm Cu = 48	12	1064.00	170.90	893.10	16.1	83.9	919.02
	14	1304.31	240.27	1064.04	18.4	81.6	1094.28
	16	1540.00	293.14	1246.86	19.0	81.0	1281.42
	18	1767.69	393.50	1374.19	22.3	77.7	1413.07
	20	2015.87	533.60	1482.27	26.5	73.5	1525.47
Stiff Cu = 96	12	1349.86	411.06	938.80	30.5	69.5	964.72
	14	1744.22	544.20	1200.02	31.2	68.8	1230.26
	16	2102.88	698.01	1404.87	33.2	66.8	1439.43
	18	2450.42	888.35	1562.07	36.3	63.7	1600.95
	20	2960.00	1121.14	1838.86	37.9	62.1	1882.06

From Table 5 it is so obviously that in soft clay the pile capacity depends on side friction (82% average over length) resistance than the end bearing (18% average over length) while for stiff clay these ratios become side friction (66% average over length) resistance than the end bearing (34% average over length). These results can be attribute to the effect of soils strength parameter which effect in the end bearing (larger by 16% as average) other than the side friction without alter the pile strength components i.e. the pile performance was still friction style. The reason can be assigned to the increasing pile length causes an increasing of the end bearing ratio for all clay soils types and decreasing for skin resistance ratio and this result can be explained from the increase of pile length will cause an increase in the overburden pressure that prevent the tip point movement leading to an increase in confined pressure at these regions. The friction side area of pile shaft leading to growing the skin resistance force other than the end bearing resistance.

Also, an important fact is obtained that is the larger pile length increases the end bearing resistance by (7%,10%,8%) for soft, firm, and stiff clay respectively. Moreover, Table 5 shows that the pile capacity were controlled by dual action of side an end pile for selected dimensions for stiff clay value while the shaft resistance become predominate in soft clay, therefore is not practical consideration to take for granted the pile in high clay strength act as floating pile. It is depicted from last two figures that the shaft resistance turn out to be lower value and end bearing larger value as pile length increased regardless soil strength changes.

Figure 18 show that the end bearing variation {(30-38)% for the stiff clay, (14-21)% for the soft, and (16-26)for firm clay}with the same pile length increasing as the soil strength is increasing, and therefore the skin resistance% {(62-70) for the stiff clay, (79-86) for the soft, and (74-84) for firm clay}is reducing as the soil strength is growing at the same pile length as shown in figure (19). The increasing in the total resistance at same pile length is distinguished as the soil strength increasing as shown in Figure 20, and also noted that the total resistance is increased as pile length is linearly increasing for the same soil strength.

Figures 21-23 show the variation of total resistance ratio and end bearing resistance ratio and skin resistance ratio with L/D, respectively. Figure 22 shows approximately linear relationship between end bearing strength parameter with the pile length diameter ratio regardless of clay soil types while skin or side friction strength parameter is less influenced by pile geometry parameter especially as strength is increased.

The tension resistance at same pile length is increased as the soil strength is increasing as shown in Figure 24 which exhibits a linear increase in tension pile capacity with increasing pile length for all clay soils. It distinguished that the tension resistance parameter is slightly changed as pile length- diameter ratio increasing for the same soil strengths as

declared in Figure 25 which show the variation of tension resistance ratio with L/D. Figures 21 and 23 show the same trend of total and end pile resistance parameters with greater length pile ratio in which both pile strength parameters turn out to be bigger their values but maintain their routine as soil type changed. But for shaft resistance parameter as display in Figure 22 the relation had so approximately a constant value communicate to each soil type. These results can be further investigation so approximately for pile behavior with different coefficients for developing a mathematical model to matching the real pile performance.

Figure 24 display the same trend of tension pile capacity with increasing pile length in which the soil strength shifted the relation line to above without changed its shape. Also, the tension resistance parameter in Figure 25 is so closely have constant value regardless of length ratio changed.

6.2.1. Important Results Regarding Clay Soils

Looking at the results of clay soils, two important remarks are observed. The first one related to the assumption of the floating idea of piles in clay soils which has some uncertainty due to a sensible amount of end bearing resistance in these soils as mentioned in the related figures that may reach to 37% of stiff clay as previously mentioned. Therefore, the partial of pile capacity shall be included in the design of such piles noting that the only exception for these piles are the bored piles of diameter 0.6 m and small length constructing in soft and firm clayey soils length (L/D less 15) after that the behavior of all piles in all clay soils become a friction-bearing actions which control the analysis and design of such piles.

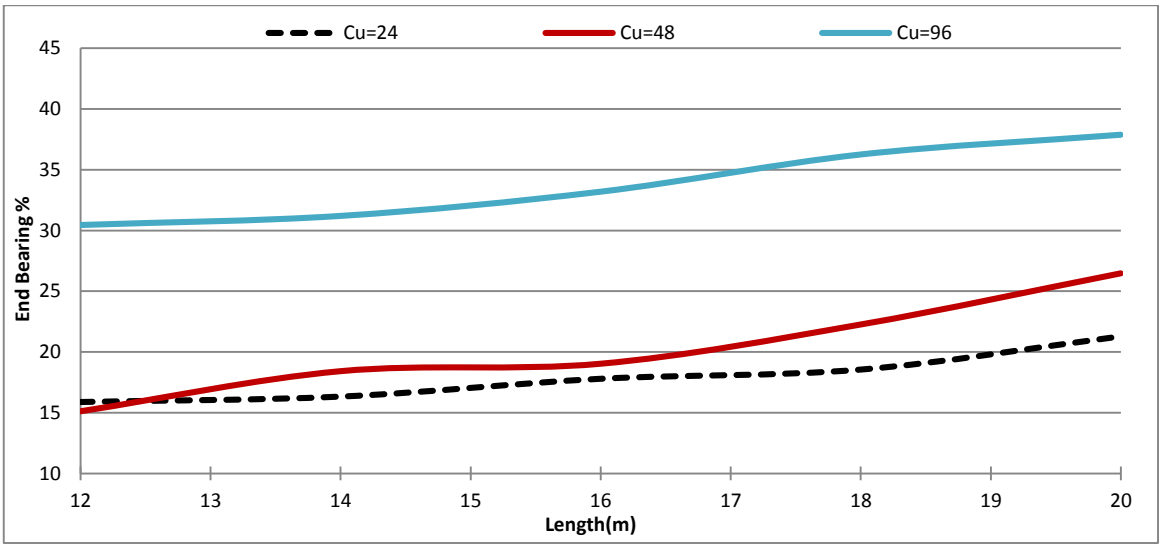

Figure 18. Relationship between end bearing % and pile length in clay soil

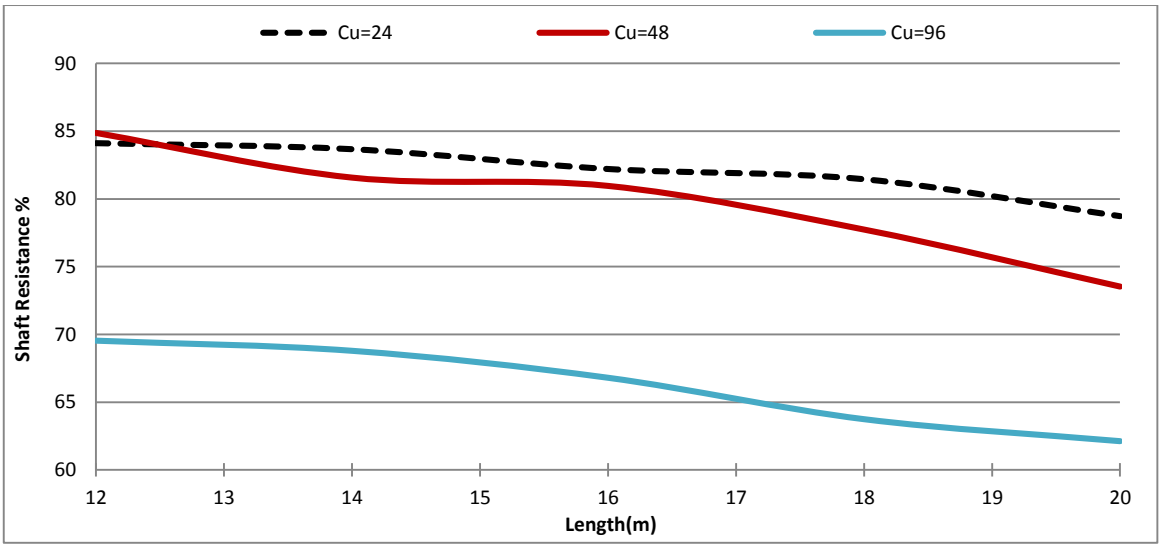

Figure 19. Relationship between Skin Resistance% and pile length in clay soil

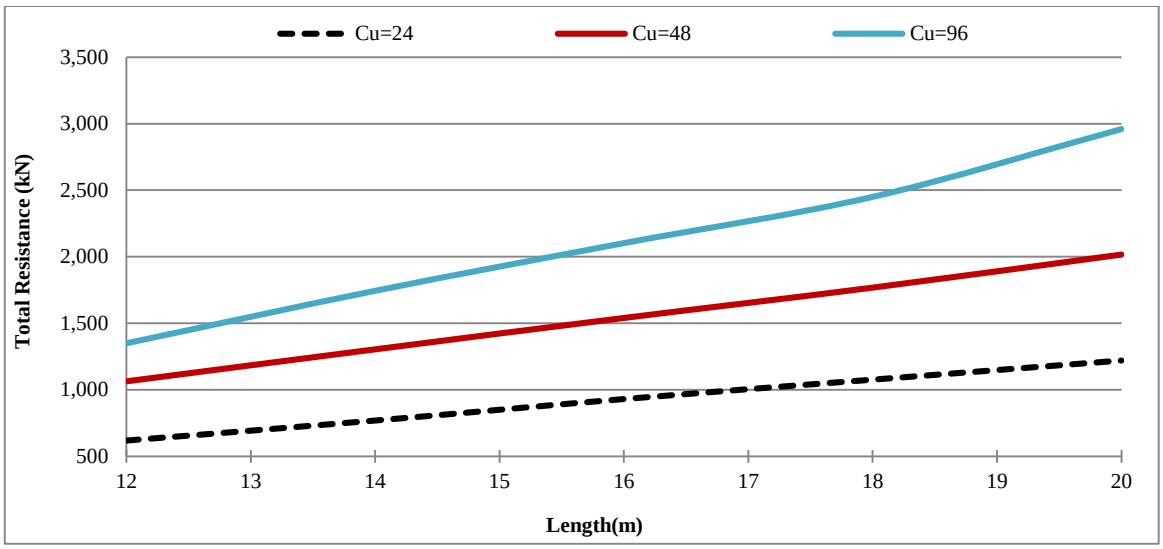

Figure 20. Variation of total resistance with pile length in clay soil

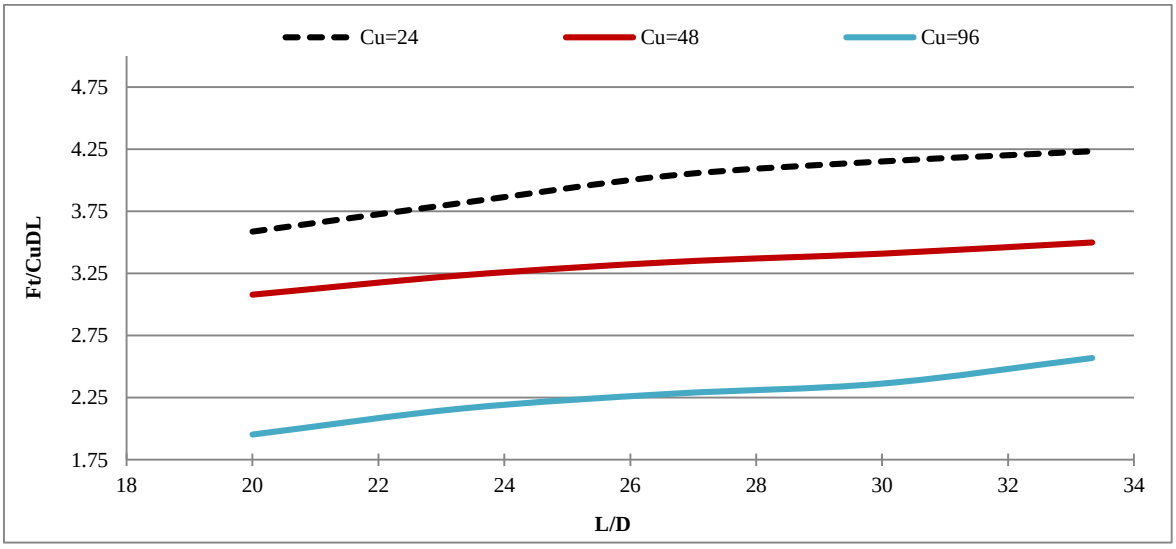

Figure 21. Variation of total resistance ratio with L/D in clay soil

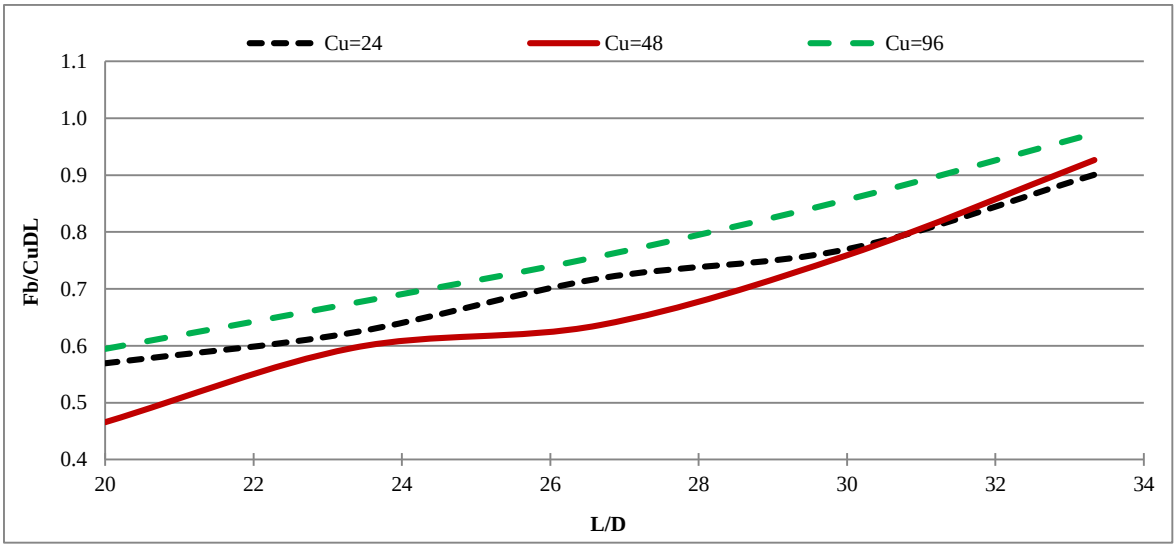

Figure 22. Variation of end bearing resistance ratio with L/D in clay soil

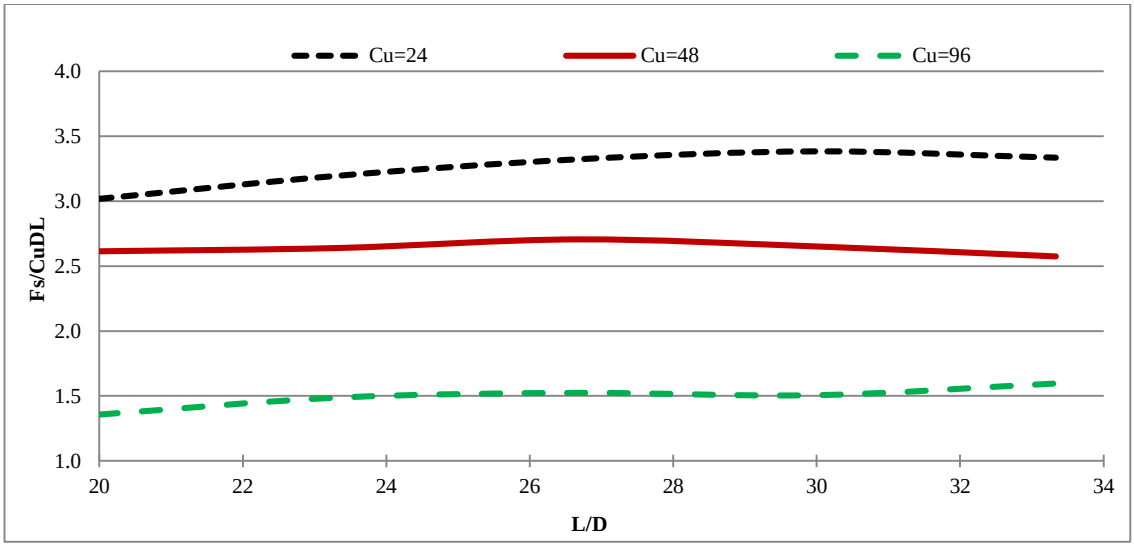

Figure 23. Variation of skin resistance ratio with L/D in clay soil

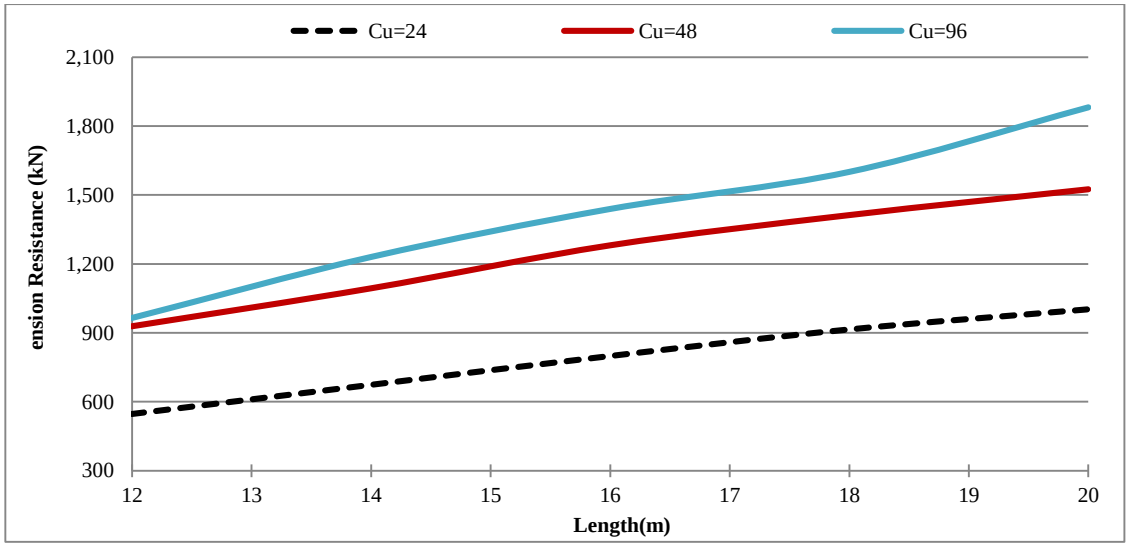

Figure 24. Variation of tension resistance with pile length in clay soil

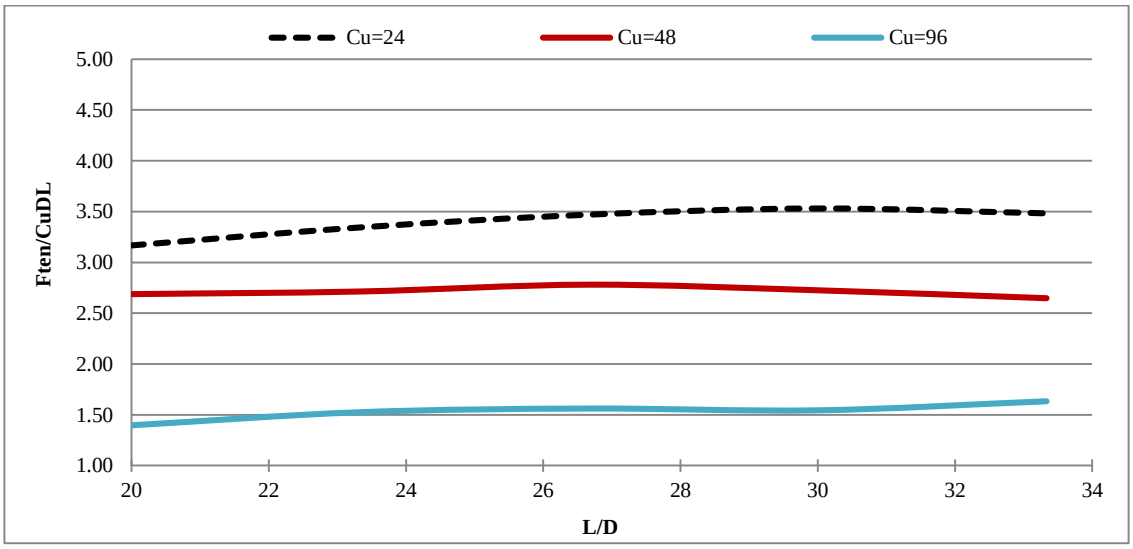

Figure 25. Variation of tension resistance ratio with L/D in clay soil

7. Conclusion

In all studied cases it's noted that the total compression resistance is increased as pile length is increasing for the same property of soil and same diameter. The total resistance at same pile length and diameter is increased as the soil strength is increasing, also noted for the same property of soil and same length that the total compression resistance is increased as pile diameter is increasing. The same situation is observed for end bearing resistance, skin resistance and tension capacity.

For bored pile in sand soil: For the pile under compression load the increasing in pile length caused a decreasing in the end bearing ratio for dense and medium sand soils types and increasing for loose sand because the increasing in pile length will causing an increasing in the friction side area of pile shaft leading to growing skin resistance force other than the end bearing resistance.

The end bearing results show the friction portion is larger than the tip point or end bearing portion for loose to medium sand soils and consequently it is valid approximately for dense sand of short length (L/D less 15).

It is economically to use piles of larger diameter than increasing their lengths for dense sand and to increasing piles lengths for loose sand.

For bored pile in clay soil: For the compression load on pile, increasing pile length cause an increase in the end bearing ratio for all clay soils types and decreasing for skin resistance and this result can be attributed to the increasing pile length will cause an increase in the overburden pressure that prevents the tip point movement leading to increase confined pressure at this regions. The friction side area of pile shaft leading to growing the skin resistance force other than the end bearing resistance.

8. Funding

This article is apart from master thesis in Basrah University/engineering College that specific at least one paper shall be published by an international journal.

9. Conflicts of Interest

The authors declare no conflict of interest.

10. References

[1] John Atkinson. "The Mechanics of Soils and Foundations, Second Edition" (16 May 2007). doi:10.1201/9781315273549.

[2] Michael Tomlinson, and John Woodward. "Pile Design and Construction Practice, Fifth Edition" (November 28, 2007). doi:10.4324/9780203964293.

[3] Coyle, H.M. and Reese, L.C. "Load transfer for axially loaded piles in clay" Journal of the Soil Mechanics and Foundations Division 92-2 (1966):1-26.

[4] Goodman, R. E., Taylor, R. L., and Brekke, T. L. "A Model for the Mechanics of Jointed Rock" Journal of the Soil Mechanics and Foundation Division, ASCE, 94, No. SM3, (May 1968): 637-659.

[5] Randolph M. F., and Wroth C. P. "Analysis of deformation of vertically loaded piles" Journal of Geotechnical and Geoenvironmental Engineering, 104 (December 1978).

[6] Van Laethem, M., E. Backx, H. Wynendaele, F. Caestecker, and G. Dhondt. "The Use of Boundary Elements to Represent the Far Field in Soil-Structure Interaction." Nuclear Engineering and Design 78, no. 3 (April 1984): 313–327. doi:10.1016/0029-5493(84)90195-x.

[7] Rojas, Eduardo, Celestino Valle, and Miguel P. Romo. "Soil-Pile Interface Model for Axially Loaded Single Piles." SOILS AND FOUNDATIONS 39, no. 4 (1999): 35–45. doi:10.3208/sandf.39.4_35.

[8] MacCabe B. A., and Lehane B. M. "Behavior of Axially Loaded Pile Groups Driven in Clayey Silt" Journal of Geotechnical and Geoenvironmental Engineering 132-3(March 2006): 401-410. doi:10.1061/(ASCE)1090-0241(2006)132:3(401).

[9] Lashkari A. "A plasticity model for sand-structure interfaces" Journal of Central South University 19-4 (2012): 1098−1108. doi:10.1007/s11771-012-1115-1.

[10] Dong -dong Pan, Qian- qing Zhang, Shan-wei Liu, and Shi-min Zhang "Analysis on Response Prediction of a Single Pile and Pile Groups Based on the Runge-Kutta Method" KSCE Journal of Civil Engineering 1 (2017) : 1-9. doi:10.1007/s12205-017-0578-x.

[11] Shengyang Feng, Xiangyang Li, Fuliang Jiang, Lin Lei, and Zhi Chen "A Nonlinear Approach for Time-Dependent Settlement nalysis of A Single Pile and Pile Groups" Soil Mechanics and Foundation Engineering 54-1 (March 2017): 7-16. doi:10.1007/s11204-017-9426-8.

[12] Hasan Ghasemzadeh, Mohsen Tarzaban, and Mohammad Mahdi "Numerical Analysis of Pile–Soil–Pile Interaction in Pile Groups with Batter Piles" Geotechnical and Geological Engineering 36-4 (January 2018): 2189–2215. doi.org/10.1007/s10706-018-0456-4.

[13] Tiago Gerheim Souza Dias, and Adam Bezuijen "Load-Transfer Method for Piles under Axial Loading and Unloading" Journal of Geotechnical and Geoenvironmental Engineering 144-1(January 2018) 04017096-1-04017096-9. doi:10.1061/(ASCE)GT.1943-5606.0001808.

[14] Md. Nafiul Haque, and Murad Y. Abu-Farsakh1 "Development of analytical models to estimate the increase in pile capacity with time (pile setup) from soil properties" Acta Geotechnica (Apri-2018): 1-25. doi:10.1007/s11440-018-0654-5.

[15] Liu Yunlong "Interpretation of Load Transfer Mechanism for Piles in Unsaturated Expansive Soils", Ph. D Thesis, Civil Engineering Department of Civil Engineering Faculty of Engineering University of Ottawa Ottawa, Ontario, Canada (February 2019). doi:10.20381/ruor-23056.

[16] Psaroudakis, E. G., G. E. Mylonakis, and N. S. Klimis. "Non-Linear Analysis of Axially Loaded Piles Using 't–z' and 'q–z' Curves." Geotechnical and Geological Engineering (February 4, 2019). doi:10.1007/s10706-019-00823-2.

[17] Bogumil Wrana "Pile load capacity–calculation methods", Studia Geotechnical et Mechanica. 37 (February 2016): 83-93. doi:10.1515/sgem-2015-0048.

[18] Hibbitt, Karlsson and Sorensen Ins., ABAQUS Theory Manual, Version 11.1, 2011.

[19] Waad U. Subber, "A Comparative Study of Interface Finite Elements in Soil-Structure Interaction Problems", M. Sc. Thesis, Department of Civil Engineering, University of Basrah, Iraq, (1996).

[20] Riyah R. Salim, "Stress Analysis of Bored Concrete Piles Using Finite Element Method", M. Sc. Thesis, Department of Civil Engineering, University of Basrah, Iraq, (2018).